

Available online at [www.sciencedirect.com](http://www.sciencedirect.com)

**jmr&t**  
Journal of Materials Research and Technology  
journal homepage: [www.elsevier.com/locate/jmrt](http://www.elsevier.com/locate/jmrt)



## Original article

# Physicomechanical properties of hydrothermally treated Japanese cedar timber and their relationships with chemical compositions



Jin-Wei Xu <sup>a,1</sup>, Cheng-Chun Li <sup>a,1</sup>, Ke-Chang Hung <sup>b</sup>, Wen-Shao Chang <sup>c</sup>,  
Jyh-Horng Wu <sup>a,\*</sup>

<sup>a</sup> Department of Forestry, National Chung Hsing University, Taichung 402, Taiwan

<sup>b</sup> Department of Wood Based Materials and Design, National Chiayi University, Chiayi 600, Taiwan

<sup>c</sup> School of Architecture, University of Sheffield, Sheffield S10 2TN, United Kingdom

## ARTICLE INFO

## Article history:

Received 14 August 2022

Accepted 15 November 2022

Available online 19 November 2022

## Keywords:

ATR-FTIR spectra

Chemical composition

Hydrothermal treatment

Japanese cedar

Physicomechanical property

## ABSTRACT

Traditional wood preservatives such as creosote, pentachlorophenol, and copper chromate arsenate have a negative impact on the environment. Therefore, it is imperative to develop environmentally friendly wood modification methods to extend the service life of wood, especially in outdoor applications. Of those modification methods, hydrothermal treatment is an attractive approach. Accordingly, the objective of the present study was to investigate the physicomechanical properties and chemical composition of hydrothermally treated Japanese cedar timber. The results revealed that the dimensional stability increased with increasing treatment temperature and duration. However, the flexural properties were decreased, which may limit the use of wood in structural applications. To understand how Japanese cedar timber responds to hydrothermal treatment, Spearman's correlation test between physicomechanical properties and second derivative attenuated total reflectance-Fourier transform infrared (ATR-FTIR) spectra was conducted. The results demonstrated that almost all physicomechanical properties were more correlated with hemicellulose and cellulose than lignin, suggesting the importance of polysaccharide degradation during hydrothermal treatment. The volume shrinkage and water absorption were more correlated with lignin than with hemicellulose and cellulose. Additionally, among all hydrothermally treated timbers, the timber processed at 200 °C for 8 h not only increases the dimensional stability and hydrophobicity of timber but also retains  $\geq 80\%$  of its flexural strength.

© 2022 The Author(s). Published by Elsevier B.V. This is an open access article under the CC BY-NC-ND license (<http://creativecommons.org/licenses/by-nc-nd/4.0/>).

\* Corresponding author.

E-mail address: [eric@nchu.edu.tw](mailto:eric@nchu.edu.tw) (J.-H. Wu).

<sup>1</sup> These authors contributed equally to this work.

<https://doi.org/10.1016/j.jmrt.2022.11.092>

2238-7854/© 2022 The Author(s). Published by Elsevier B.V. This is an open access article under the CC BY-NC-ND license (<http://creativecommons.org/licenses/by-nc-nd/4.0/>).

## 1. Introduction

Wood has been used for architecture, decoration, and furniture for many applications due to its excellent properties, such as superior strength-to-weight, low thermal conduction, processability, and aesthetic appearance [1–3]. However, wood is easily damaged by various biodegrading organisms and microorganisms, including fungi, bacteria, termites, insects, and marine microorganisms, because of its hygroscopicity [4]. Meanwhile, the hygroscopicity also leads to dimensional instability, which limits the use of wood in many applications [5,6]. In general, wood is commonly treated with preservatives to achieve protection against moisture fluctuation and microorganisms. However, traditional wood preservatives such as creosote, pentachlorophenol, and copper chromate arsenate have a negative impact on the environment. Therefore, various environmentally friendly physical and chemical modifications, including heat treatment [1], siloxane modification [7], furfurylation [8], acetylation [9], and hydrolysed feather keratin modification [10], have been conducted to extend the service life of wood, especially in outdoor applications. Among these modifications, hydrothermal treatment, as an effective and environmentally friendly heat treatment method, has attracted much attention [11,12].

Heat treatment mainly degrades hydrophilic hemicellulose and prevent moisture from entering the wood, thereby improving dimensional stability and prolonging service life of wood [13,14]. In addition, hemicellulose is generally considered as an important nutritive source and a major key to the development of wood rotting fungi [15]. Thus, heat-treated wood is more resistant to degradation by wood-rotting fungi. Furthermore, the heat treatment of wood has been an important research topic for decades, and several industrial processes such as ThermoWood, Rectification, Le Bois Perdure, ThermoVuoto, etc. have also been developed [16]. These treatments are typically carried out in the temperature range of 160–260 °C, where lower temperatures do not reduce the hygroscopicity of wood, while higher temperatures severely degrade the wood composition, leading to a reduction in mechanical properties [17–19]. Meanwhile, heat treatment can be conducted in different media, including air, nitrogen, water, steam, and oil [1,20]. Therefore, different heat treatment conditions and media will lead to different chemical degradation, which further results in a change in the properties of wood [18]. Additionally, heat treatment conducted in air, nitrogen, and oil not only causes the dehydration, hydrolysis, oxidation, and decarboxylation of principal components (i.e., cellulose, hemicellulose, and lignin) but also creates additional covalent bonds and hydrogen bonding, which reduce the equilibrium moisture content (EMC) and volumetric swelling by inducing repolymerization or rearrangement reactions [21].

Although the physicomechanical properties and chemical degradation of hydrothermal treatment have been implicated in the scientific literature, to the best of our knowledge, no study has analysed these changes with high pressure (1.52 MPa) hydrothermal treatment. Furthermore, analysing property changes in relation to chemical degradation under different treatment conditions is important for a better

understanding of the processes involved. Therefore, this study investigated the physicomechanical properties and chemical degradation of hydrothermal treatment and further explored their correlation by Spearman's correlation to understand the role of treatment conditions, especially under a high-pressure water vapour state.

## 2. Materials and methods

### 2.1. Materials

Japanese cedar (*Cryptomeria japonica* D. Don) (40–45 years old) timber was supplied by Jang Chang Lumber Industry Co., Ltd. (Hsinchu, Taiwan). Flat-sawn timbers with dimensions of 3600 mm × 136 mm × 26 mm and an average density of 396 kg/m<sup>3</sup> were prepared from conventionally kiln-dried wood with an average moisture content of 14%. Forty-five timbers without visible defects were chosen for the present experiment, and each timber was cut into 7 subsamples (500 mm × 136 mm × 26 mm). To reduce the variability among test groups, as shown in Fig. 1, those subsamples were divided into 16 groups, and each group contained 15 test specimens. Before hydrothermal treatment, all specimens were conditioned at 20 °C and 65% relative humidity (RH) for at least 2 weeks.

### 2.2. Hydrothermal treatment of Japanese cedar timber

A semi-industrial reactor equipped with a thermocouple and pressure sensors (San Neng Ltd., Chiayi, Taiwan) was used for the hydrothermal treatment of Japanese cedar timber. The timber and a proper amount of water were placed in the tank without contact with each other. Subsequently, the timbers were heated from room temperature to the desired temperature (160, 180, 200, 220, and 240 °C) with a heating rate of 3 °C/min, which was maintained for 4, 8, and 16 h, respectively. The timbers were then cooled to room temperature over 12 h.

### 2.3. Determination of untreated and hydrothermally treated Japanese cedar timbers

To determine the physicomechanical properties of untreated and hydrothermally treated Japanese cedar timbers, several determinations, including air-dry density, mass loss, volume shrinkage, water absorption, total volume swelling (TVS), flexural properties, equilibrium moisture content (EMC), moisture excluding efficiency (MEE), and volumetric swelling coefficient (S), were conducted. In brief, the air-dry density and EMC of cubic specimens with dimensions of 26 mm × 26 mm × 26 mm were measured according to the Chinese National Standard CNS 451 [22] and CNS 452 [23], respectively. The mass loss (%) was calculated as follows:  $(1 - W_1/W_0) \times 100$ , where  $W_0$  and  $W_1$  were the mass (g) of untreated and hydrothermally treated Japanese cedar timber (500 mm × 136 mm × 26 mm), respectively. The volume shrinkage (%) was calculated by equation  $(1 - (W_1/\rho_1)/(W_0/\rho_0)) \times 100$ , where  $W_0$  and  $W_1$  represent the mass (g) of untreated and hydrothermally treated Japanese cedar timber

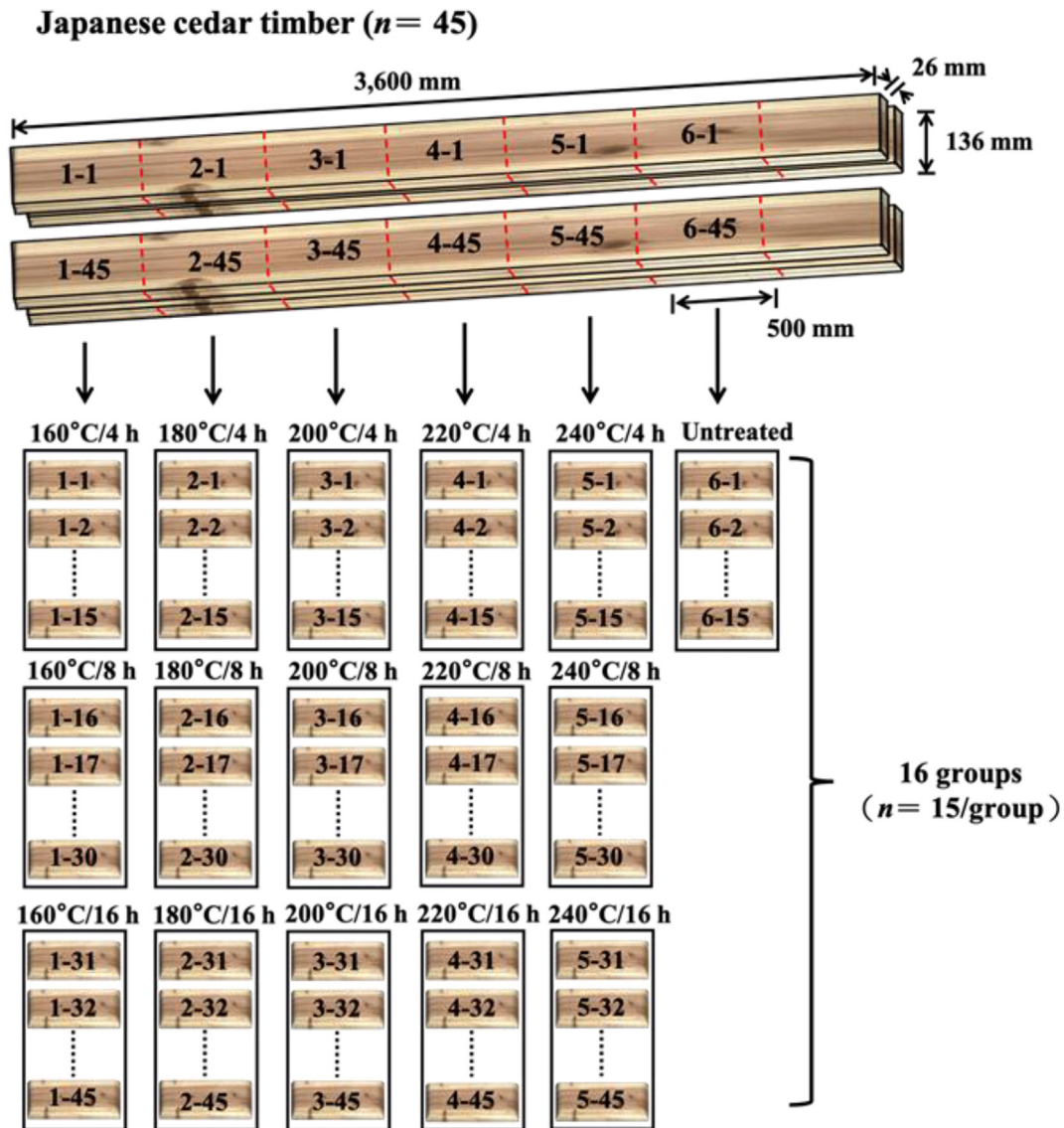


Fig. 1 – Schematic diagram for sample preparation and grouping of Japanese cedar timber.

and  $\rho_0$  and  $\rho_1$  represent the density ( $\text{g}/\text{cm}^3$ ) of untreated and hydrothermally treated Japanese cedar timber. The water absorption and TVS were measured according to CNS 14927 [24]. The MEE and S were measured according to ASTM D1037 [25]. The flexural properties were determined according to CNS 454 [26] by a universal testing machine (Shimadzu AG-10 kNX, Tokyo, Japan). The modulus of rupture (MOR) and modulus of elasticity (MOE) of the timbers with dimensions of 500 mm  $\times$  136 mm  $\times$  26 mm were determined through the three-point flexural test at a loading speed of 5 mm/min and a span of 364 mm. All samples were conditioned at 20 °C and 65% RH for two weeks prior to testing, and 15 replicate specimens were tested for each group. In addition, for the measurements of EMC, MEE, and S, the samples were also conditioned at 20 °C/75% RH and 20 °C/85% RH for two weeks.

#### 2.4. Measurement of surface colour

The colour of untreated and hydrothermally treated Japanese cedar timber was measured by a colour and colour difference meter (CM-3600d, Minolta, Tokyo, Japan) under a  $D_{65}$  light source with a test window diameter of 8 mm. The colour parameters  $L^*$ ,  $a^*$ , and  $b^*$  of all specimens were obtained directly from the colorimeter. Based on the CIE  $L^*a^*b^*$  colour system,  $L^*$  is the value on the white/black axis,  $a^*$  is the value on the red/green axis,  $b^*$  is the value on the yellow/blue axis, and the  $\Delta E^*$  value is the colour difference ( $\Delta E^* = [(\Delta L^*)^2 + (\Delta a^*)^2 + (\Delta b^*)^2]^{1/2}$ ).

#### 2.5. ATR-FTIR spectral measurements

Attenuated total reflectance-Fourier transform infrared (ATR-FTIR) spectra of untreated and hydrothermally treated

**Table 1 – Set point parameters, mass loss, density, volume shrinkage, water absorption, and total volume swelling (TVS) of untreated and hydrothermally treated Japanese cedar timber.**

Sample code	Temperature (°C)	Duration (h)	Pressure (MPa)	Mass loss (%)	Density (kg/m <sup>3</sup> )	Volume shrinkage (%)	24 h Water soaking	
							Water absorption (%)	TVS (%)
Untreated	–	–	–	–	429 ± 56	–	151 ± 27	11.4 ± 1.4
160 °C/4 h	160	4	0.22	2.7 ± 0.8 <sup>D,b</sup>	376 ± 38 <sup>A,a,ns</sup>	1.12 ± 0.12 <sup>A,a</sup>	188 ± 27 <sup>A,a,**</sup>	11.9 ± 1.4 <sup>A,a,ns</sup>
160 °C/8 h	160	8	0.23	3.5 ± 0.9 <sup>D,a</sup>	408 ± 66 <sup>A,a,ns</sup>	1.08 ± 0.14 <sup>A,a</sup>	175 ± 31 <sup>A,a,*</sup>	12.4 ± 1.5 <sup>A,a,*</sup>
160 °C/16 h	160	16	0.25	3.5 ± 0.8 <sup>D,a</sup>	410 ± 62 <sup>A,a,ns</sup>	1.02 ± 0.19 <sup>A,a</sup>	150 ± 36 <sup>A,a,ns</sup>	12.1 ± 1.5 <sup>A,a,ns</sup>
180 °C/4 h	180	4	0.25	3.4 ± 0.9 <sup>D,b</sup>	387 ± 46 <sup>A,a,ns</sup>	1.09 ± 0.14 <sup>A,a</sup>	175 ± 28 <sup>A,a,*</sup>	12.7 ± 1.3 <sup>A,a,*</sup>
180 °C/8 h	180	8	0.25	3.6 ± 0.8 <sup>D,b</sup>	409 ± 68 <sup>A,a,ns</sup>	1.04 ± 0.15 <sup>A,a</sup>	149 ± 35 <sup>AB,ab,ns</sup>	12.1 ± 1.3 <sup>A,a,*</sup>
180 °C/16 h	180	16	0.35	4.6 ± 0.5 <sup>D,a</sup>	412 ± 63 <sup>A,a,ns</sup>	1.04 ± 0.17 <sup>A,a</sup>	144 ± 28 <sup>B,a,ns</sup>	9.3 ± 1.3 <sup>B,b,**</sup>
200 °C/4 h	200	4	0.33	4.2 ± 3.0 <sup>C,c</sup>	383 ± 43 <sup>A,a,ns</sup>	1.07 ± 0.14 <sup>A,a</sup>	181 ± 30 <sup>A,b,**</sup>	9.7 ± 1.5 <sup>A,b,**</sup>
200 °C/8 h	200	8	0.36	5.4 ± 1.4 <sup>C,b</sup>	398 ± 56 <sup>A,a,ns</sup>	1.02 ± 0.14 <sup>A,a</sup>	123 ± 36 <sup>B,b,*</sup>	8.7 ± 1.4 <sup>A,b,**</sup>
200 °C/16 h	200	16	0.68	8.7 ± 0.6 <sup>C,a</sup>	397 ± 59 <sup>A,a,ns</sup>	1.04 ± 0.18 <sup>A,a</sup>	109 ± 31 <sup>B,a,**</sup>	5.5 ± 0.9 <sup>B,c,d,**</sup>
220 °C/4 h	220	4	0.46	6.4 ± 0.8 <sup>B,c</sup>	368 ± 46 <sup>A,a,ns</sup>	1.11 ± 0.13 <sup>A,a</sup>	161 ± 23 <sup>A,b,ns</sup>	8.6 ± 0.9 <sup>B,b,**</sup>
220 °C/8 h	220	8	0.73	8.7 ± 1.9 <sup>B,b</sup>	381 ± 53 <sup>A,a,ns</sup>	0.99 ± 0.13 <sup>A,a</sup>	120 ± 32 <sup>B,b,**</sup>	7.1 ± 1.0 <sup>B,c,**</sup>
220 °C/16 h	220	16	1.03	13.0 ± 0.6 <sup>B,a</sup>	373 ± 55 <sup>A,a,ns</sup>	1.05 ± 0.18 <sup>A,a</sup>	136 ± 44 <sup>AB,a,ns</sup>	6.4 ± 0.8 <sup>B,c,**</sup>
240 °C/4 h	240	4	0.63	28.4 ± 2.0 <sup>A,c</sup>	363 ± 50 <sup>A,a,ns</sup>	1.08 ± 0.14 <sup>A,a</sup>	163 ± 31 <sup>A,b,ns</sup>	7.1 ± 0.9 <sup>A,c,**</sup>
240 °C/8 h	240	8	1.24	14.3 ± 0.8 <sup>A,b</sup>	365 ± 48 <sup>A,a,ns</sup>	1.04 ± 0.13 <sup>A,a</sup>	135 ± 31 <sup>A,b,ns</sup>	6.0 ± 0.8 <sup>B,c,**</sup>
240 °C/16 h	240	16	1.52	23.6 ± 1.5 <sup>A,a</sup>	352 ± 72 <sup>A,a,ns</sup>	1.00 ± 0.23 <sup>A,a</sup>	136 ± 44 <sup>A,a,ns</sup>	4.7 ± 1.0 <sup>C,d,**</sup>

Values are mean ± SD (n = 15). Different capital and lowercase letters within a column indicate significant difference among various durations (p < 0.05) and temperatures (p < 0.05), respectively. ns: non-significant; \*: p < 0.05; \*\*: p < 0.01, compared with untreated Japanese cedar timber.

Japanese cedar timber were recorded on a Spectrum 100 FTIR spectrometer (PerkinElmer, Buckinghamshire, UK) equipped with a deuterated triglycine sulfate (DTGS) detector and a MIRacle ATR accessory (Pike Technologies, Madison, WI, USA). The spectra were collected by adding 32 scans at a resolution of 4 cm<sup>-1</sup> in the range from 650 to 4000 cm<sup>-1</sup>.

**2.6. Principal component analysis of untreated and hydrothermally treated Japanese cedar timber**

Principal component analysis (PCA) identifies directions (principal components, PCs) along which the variance of the data is maximal [27]. The effect of this process is a concentration of the sources of variability of the dataset into a few PCs. Plots of the PC scores (projection onto PC axes) against one another can reveal clustering or structure in the dataset. For data analysis, the data of physicochemical properties were normalized, and then the data were used for PCA, and the factor loadings were plotted.

**2.7. Spearman's correlation analysis**

Spearman correlations were used to determine relationships between physicochemical properties (i.e., mass loss, density, water absorption, volume shrinkage, S, TVS, EMC, colour parameters, MOE, and MOR) and between these properties and second derivative ATR-FTIR spectra. The importance of the identified feature was based on the results from Spearman's correlation matrix, which was made in R (version 4.0.4, The R Foundation for Statistical Computing, Vienna, Austria) using the corrplot package [28].

**2.8. Statistical analysis**

All results are expressed as the mean ± standard deviation (SD). The significance of differences was calculated using

Scheffe's test or Student's t-test, and p values <0.05 were considered to be significant.

**3. Results and discussion**

**3.1. Physicochemical properties of untreated and hydrothermally treated Japanese cedar timbers**

The set point parameters, including mass loss, density, volume shrinkage, water absorption, and TVS, of untreated and hydrothermally treated Japanese cedar timbers are summarized in Table 1. The mass losses of hydrothermally treated Japanese cedar timber were in the range of 2.7–23.6%, which increased with increasing treatment temperature and duration. In general, the hydrolysis of biomass is started by hydronium ions (H<sub>3</sub>O<sup>+</sup>), which act as acid catalysts and hydrolyse principal components to mainly monomers [29]. Thus, in this study, hydronium ions increased with increasing treatment temperature and duration, which was consistent with the report by Rissanen et al. [30].

Additionally, the density and volume shrinkage of hydrothermally treated Japanese cedar timber exhibited no significant difference compared to the untreated Japanese cedar timber. However, after 24 h of water immersion, the water absorption of the timbers was significantly influenced by the treatment temperature and duration. The water absorptions of untreated and hydrothermal treatment timbers were 151% and 109–188%, respectively. Among these values, the 160 °C/4 h and 200 °C/16 h groups exhibited the highest and lowest water absorptions, respectively. Generally, the water absorption of hydrothermally treated Japanese cedar timbers decreased with increasing treatment temperature and duration, except for 240 °C/4–16 h and 220 °C/16 h. This result may be related to the change in timber volume. The slight increase in water absorption after hydrothermal treatment may be

related to the degradation of hydrophobic lignin and the formation of microcracks, which allow easier entrance of water into the cell wall [31]. Wentzel et al. [32,33] also observed lignin degradation and microcrack formation in *Eucalyptus nitens* specimens under hydrothermal treatment at 160 °C. Meanwhile, because the water absorption did not increase with increasing treatment temperature and duration, the microcracks did not increase due to the rising temperature and duration, which was similar to the report of Bernabei and Salvatici [34]. In contrast, the water absorption decreased with increasing treatment temperature and duration, which was attributed to the hydrothermal treatment removing the accessible OH groups, leading to a reduction in water absorption. Moreover, similar to water absorption, the trend of TVS also increased with increasing treatment temperature and duration, reaching a maximum at 180 °C/4 h, and then decreased as the treatment temperature or duration increased. This result may also be related to the aforementioned degradation of lignin, formation of microcracks, and reduction of accessible OH groups.

Table 2 presents the EMC, MEE, and S of untreated and hydrothermally treated Japanese cedar timbers under 20 °C/65% RH, 20 °C/75% RH, and 20 °C/85% RH conditions. For each conditioning environment, the EMC presented a similar trend. The hydrothermal treatment at 160–240 °C decreased the EMC values by 2.3–11.5%, depending on the treatment temperature and duration. In contrast, the MEE increased with increasing treatment temperature and duration. Comparing the timber treated at 240 °C for 16 h (240 °C/16 h) to the untreated timber, the MEE increased 77, 72, and 69% under 20 °C/65% RH, 20 °C/75% RH, and 20 °C/85% RH, respectively. This phenomenon is attributed mainly to the reduction of the accessible OH groups by hydrothermal treatment, resulting in a decrease in EMC. Meanwhile, cellulose aggregation and hydrogen bonding may also decrease the hygroscopicity. However, as shown in Table 2, the MEE decreased with increasing relative humidity. In other words, the number of accessible OH groups may increase with increasing relative humidity. The results implied that the destroyed sorption sites may be restored to form new accessible OH groups by mechanical relaxation, which was also reported by Altgen et al. [35]. Additionally, similar to TVS, the S of hydrothermally treated Japanese cedar timber increased with increasing treatment temperature and duration, reaching a maximum at 160 °C/16 h (20 °C/65% RH), 180 °C/4 h (20 °C/75% RH), and 180 °C/8 h (20 °C/85% RH), and then generally decreased as the temperature and duration increased. Meanwhile, S is also affected by mechanical relaxation and softening of the amorphous cell wall matrix polymers; thus, increasing the relative humidity will promote the rearrangement of the matrix polymers, leading to a higher S, consistent with the report of Endo et al. [36].

The colour variation and flexural properties of untreated and hydrothermally treated Japanese cedar timbers are shown in Table 3. The L\*, a\*, and b\* of untreated and hydrothermally treated Japanese cedar timbers ranged from 34.8 to 67.6, 7.9 to 10.5, and 13.3 to 21.4, respectively. The L\*, a\*, and b\* values decreased with increasing treatment temperature and duration. These results revealed that the surface colour of Japanese cedar timbers was darker during hydrothermal treatment. A similar result was also reported by Yang et al.

**Table 2 – Equilibrium moisture content (EMC), moisture excluding efficiency (MEE), and volumetric swelling coefficient (S) of untreated and hydrothermally treated Japanese cedar timber under 20 °C/65% RH, 20 °C/75% RH, and 20 °C/85% RH conditions.**

Sample code	EMC (%)			MEE (%)			S (%)		
	65% RH	75% RH	85% RH	65% RH	75% RH	85% RH	65% RH	75% RH	85% RH
Untreated	14.0 ± 0.4	15.7 ± 0.4	16.6 ± 0.4	–	–	–	3.8 ± 1.1	4.4 ± 1.0	4.9 ± 1.1
160 °C/4 h	7.7 ± 0.7 <sup>A,a**</sup>	10.9 ± 0.5 <sup>A,a**</sup>	14.4 ± 0.8 <sup>A,a**</sup>	45 ± 5 <sup>A,c</sup>	30 ± 3 <sup>C,d</sup>	13 ± 5 <sup>C,e</sup>	3.3 ± 0.9 <sup>C,ans</sup>	4.8 ± 0.8 <sup>B,bs</sup>	5.2 ± 0.8 <sup>A,a**</sup>
160 °C/8 h	7.3 ± 0.6 <sup>A,a**</sup>	9.7 ± 0.7 <sup>B,b**</sup>	12.3 ± 0.8 <sup>B,a**</sup>	48 ± 4 <sup>A,c</sup>	38 ± 4 <sup>B,b</sup>	26 ± 5 <sup>B,d</sup>	4.5 ± 0.6 <sup>B,a**</sup>	5.8 ± 0.8 <sup>A,a**</sup>	6.1 ± 0.9 <sup>A,b**</sup>
160 °C/16 h	7.2 ± 0.3 <sup>A,a**</sup>	8.8 ± 0.4 <sup>C,b**</sup>	10.2 ± 0.3 <sup>C,b**</sup>	48 ± 2 <sup>A,e</sup>	44 ± 2 <sup>A,c</sup>	38 ± 2 <sup>A,d</sup>	5.2 ± 0.7 <sup>A,a**</sup>	5.5 ± 0.7 <sup>A,a**</sup>	5.7 ± 0.5 <sup>A,a**</sup>
180 °C/4 h	7.9 ± 0.3 <sup>A,a**</sup>	10.8 ± 1.6 <sup>B,a**</sup>	11.7 ± 0.5 <sup>C,b**</sup>	44 ± 2 <sup>C,c</sup>	31 ± 6 <sup>A,d</sup>	29 ± 3 <sup>B,d</sup>	3.9 ± 1.0 <sup>A,ans</sup>	6.5 ± 1.1 <sup>A,a**</sup>	5.9 ± 0.9 <sup>B,a**</sup>
180 °C/8 h	7.0 ± 0.7 <sup>B,a**</sup>	11.5 ± 0.6 <sup>A,a**</sup>	12.7 ± 0.9 <sup>A,a**</sup>	50 ± 5 <sup>B,c</sup>	26 ± 4 <sup>B,c</sup>	23 ± 5 <sup>B,d</sup>	4.4 ± 0.8 <sup>A,a**</sup>	5.7 ± 0.9 <sup>B,a**</sup>	7.8 ± 1.3 <sup>A,a**</sup>
180 °C/16 h	6.4 ± 0.4 <sup>C,b**</sup>	10.9 ± 0.4 <sup>AB,a**</sup>	11.1 ± 0.3 <sup>B,a**</sup>	54 ± 3 <sup>A,d</sup>	30 ± 2 <sup>B,d</sup>	31 ± 2 <sup>A,e</sup>	3.2 ± 0.6 <sup>B,c**</sup>	5.2 ± 0.6 <sup>B,c**</sup>	4.6 ± 0.7 <sup>C,ns</sup>
200 °C/4 h	7.8 ± 0.3 <sup>A,a**</sup>	9.7 ± 0.8 <sup>AB,b**</sup>	10.3 ± 0.6 <sup>A,c**</sup>	44 ± 2 <sup>C,c</sup>	38 ± 5 <sup>B,c</sup>	38 ± 4 <sup>B,c</sup>	3.3 ± 0.7 <sup>A,ans</sup>	4.5 ± 0.6 <sup>B,ns</sup>	3.7 ± 0.6 <sup>B,ns</sup>
200 °C/8 h	6.9 ± 1.1 <sup>B,a**</sup>	9.3 ± 1.0 <sup>A,b**</sup>	11.1 ± 0.9 <sup>A,b**</sup>	51 ± 8 <sup>B,c</sup>	41 ± 5 <sup>B,b</sup>	33 ± 5 <sup>B,c</sup>	3.8 ± 0.8 <sup>A,abns</sup>	5.2 ± 1.0 <sup>A,ab*</sup>	6.5 ± 1.5 <sup>A,b**</sup>
200 °C/16 h	5.3 ± 0.4 <sup>C,c**</sup>	8.5 ± 0.5 <sup>B,b**</sup>	9.3 ± 1.1 <sup>B,c**</sup>	63 ± 3 <sup>A,c</sup>	45 ± 3 <sup>A,c</sup>	44 ± 6 <sup>A,c</sup>	2.4 ± 0.6 <sup>B,d**</sup>	3.7 ± 0.8 <sup>C,b**</sup>	3.5 ± 0.9 <sup>B,c**</sup>
220 °C/4 h	6.1 ± 0.3 <sup>AB,b**</sup>	8.8 ± 0.7 <sup>A,c**</sup>	9.2 ± 0.4 <sup>A,d**</sup>	57 ± 2 <sup>C,b</sup>	44 ± 5 <sup>C,b</sup>	44 ± 2 <sup>C,b</sup>	3.5 ± 0.4 <sup>B,ans</sup>	4.5 ± 0.8 <sup>AB,ns</sup>	4.4 ± 0.5 <sup>A,bns</sup>
220 °C/8 h	5.1 ± 0.4 <sup>B,b**</sup>	6.8 ± 0.8 <sup>B,c**</sup>	7.6 ± 0.7 <sup>B,c**</sup>	64 ± 3 <sup>B,b</sup>	57 ± 5 <sup>B,a</sup>	54 ± 5 <sup>B,b</sup>	4.1 ± 0.8 <sup>A,abns</sup>	4.5 ± 0.7 <sup>A,ns</sup>	4.4 ± 0.7 <sup>A,ns</sup>
220 °C/16 h	4.2 ± 0.3 <sup>C,d**</sup>	5.6 ± 0.4 <sup>C,c**</sup>	6.2 ± 0.3 <sup>C,d**</sup>	70 ± 2 <sup>A,b</sup>	64 ± 3 <sup>A,b</sup>	63 ± 2 <sup>A,b</sup>	4.0 ± 0.7 <sup>A,bns</sup>	4.8 ± 0.7 <sup>A,ans</sup>	4.4 ± 0.8 <sup>A,bns</sup>
240 °C/4 h	5.2 ± 0.4 <sup>A,c**</sup>	6.7 ± 0.4 <sup>A,d**</sup>	8.1 ± 0.5 <sup>A,e**</sup>	63 ± 3 <sup>C,a</sup>	57 ± 2 <sup>C,a</sup>	51 ± 3 <sup>C,a</sup>	3.4 ± 0.6 <sup>A,bns</sup>	3.8 ± 0.6 <sup>AB,c**</sup>	3.4 ± 0.7 <sup>A,c**</sup>
240 °C/8 h	4.3 ± 0.3 <sup>B,c**</sup>	6.2 ± 0.6 <sup>B,c**</sup>	6.2 ± 0.5 <sup>B,d**</sup>	70 ± 2 <sup>B,a</sup>	61 ± 4 <sup>B,a</sup>	62 ± 3 <sup>B,a</sup>	3.7 ± 0.9 <sup>A,bns</sup>	4.2 ± 0.9 <sup>A,ns</sup>	3.9 ± 0.8 <sup>A,ns</sup>
240 °C/16 h	3.3 ± 0.4 <sup>C,d**</sup>	4.5 ± 0.4 <sup>C,e**</sup>	5.1 ± 0.4 <sup>C,e**</sup>	77 ± 2 <sup>A,a</sup>	72 ± 2 <sup>A,a</sup>	69 ± 2 <sup>A,a</sup>	3.7 ± 1.0 <sup>A,b,ns</sup>	3.4 ± 1.2 <sup>B,b**</sup>	4.0 ± 1.1 <sup>A,b,c**</sup>

Values are mean ± SD (n = 15). Different capital and lowercase letters within a column indicate significant difference among various durations (p < 0.05) and temperatures (p < 0.05), respectively. ns: non-significant; \*, p < 0.05; \*\*, p < 0.01, compared with untreated Japanese cedar timber.

**Table 3 – Colour parameters ( $L^*$ ,  $a^*$ ,  $b^*$ , and  $\Delta E^*$ ), modulus of elasticity (MOE), and modulus of rupture (MOR) of untreated and hydrothermally treated Japanese cedar timber.**

Sample code	CIE $L^*a^*b^*$			$\Delta E^*$	MOE (GPa)	MOR (MPa)
	$L^*$	$a^*$	$b^*$			
Untreated	67.6 ± 5.4	10.5 ± 4.0	21.4 ± 1.7	—	6.4 ± 1.3	57.8 ± 10.2
160 °C/4 h	59.9 ± 5.6 <sup>A,a,**</sup>	10.4 ± 1.4 <sup>A,a,ns</sup>	22.5 ± 1.4 <sup>A,a,*</sup>	8.4 ± 5.0 <sup>B,d</sup>	6.2 ± 1.2 <sup>A,a,ns</sup>	51.1 ± 8.0 <sup>A,a,*</sup>
160 °C/8 h	56.0 ± 5.6 <sup>A,a,**</sup>	10.8 ± 0.9 <sup>A,a,ns</sup>	21.5 ± 1.5 <sup>A,a,ns</sup>	11.8 ± 5.6 <sup>AB,c</sup>	6.1 ± 1.0 <sup>A,a,ns</sup>	59.3 ± 12.6 <sup>A,ab,ns</sup>
160 °C/16 h	55.2 ± 4.4 <sup>A,a,**</sup>	10.1 ± 1.0 <sup>A,a,ns</sup>	21.3 ± 5.2 <sup>A,a,ns</sup>	13.7 ± 3.1 <sup>A,d</sup>	7.0 ± 1.2 <sup>A,a,ns</sup>	61.1 ± 13.2 <sup>A,a,ns</sup>
180 °C/4 h	56.7 ± 6.2 <sup>A,ab,**</sup>	10.1 ± 0.8 <sup>A,a,ns</sup>	21.5 ± 1.3 <sup>B,a,ns</sup>	11.1 ± 6.0 <sup>A,cd</sup>	6.7 ± 0.8 <sup>A,a,ns</sup>	54.3 ± 8.8 <sup>A,a,ns</sup>
180 °C/8 h	53.9 ± 6.2 <sup>A,a,**</sup>	10.4 ± 0.9 <sup>A,a,ns</sup>	22.0 ± 2.0 <sup>AB,a,ns</sup>	14.1 ± 5.7 <sup>A,c</sup>	6.6 ± 1.4 <sup>A,a,ns</sup>	61.8 ± 14.9 <sup>A,a,ns</sup>
180 °C/16 h	52.8 ± 5.8 <sup>A,a,**</sup>	10.1 ± 0.7 <sup>A,a,ns</sup>	23.2 ± 2.0 <sup>A,ab,ns</sup>	15.3 ± 5.3 <sup>A,d</sup>	6.1 ± 1.3 <sup>A,ab,ns</sup>	50.7 ± 11.9 <sup>A,a,*</sup>
200 °C/4 h	53.1 ± 4.1 <sup>A,bc,**</sup>	10.0 ± 0.5 <sup>A,a,ns</sup>	22.1 ± 1.6 <sup>A,a,ns</sup>	14.7 ± 4.0 <sup>B,bc</sup>	6.2 ± 0.9 <sup>AB,a,ns</sup>	53.4 ± 9.9 <sup>A,a,ns</sup>
200 °C/8 h	46.2 ± 4.1 <sup>B,b,**</sup>	10.1 ± 0.7 <sup>A,a,ns</sup>	21.6 ± 2.1 <sup>A,a,ns</sup>	21.5 ± 4.1 <sup>A,b</sup>	6.9 ± 1.1 <sup>A,a,ns</sup>	47.2 ± 12.8 <sup>A,bc,**</sup>
200 °C/16 h	44.5 ± 3.5 <sup>B,b,**</sup>	10.0 ± 0.6 <sup>A,a,ns</sup>	21.1 ± 1.9 <sup>A,ab,ns</sup>	23.2 ± 3.6 <sup>A,c</sup>	5.2 ± 1.1 <sup>B,b,*</sup>	31.6 ± 8.9 <sup>B,b,**</sup>
220 °C/4 h	50.1 ± 3.5 <sup>A,c,**</sup>	10.4 ± 0.8 <sup>A,a,ns</sup>	23.0 ± 1.3 <sup>A,a,**</sup>	17.6 ± 3.5 <sup>C,b</sup>	6.3 ± 0.8 <sup>A,a,ns</sup>	45.7 ± 8.0 <sup>A,ab,**</sup>
220 °C/8 h	43.4 ± 3.9 <sup>B,bc,**</sup>	10.2 ± 0.8 <sup>AB,a,ns</sup>	20.9 ± 2.5 <sup>B,a,ns</sup>	24.3 ± 3.9 <sup>B,ab</sup>	6.3 ± 1.4 <sup>A,a,ns</sup>	40.0 ± 12.5 <sup>A,c,**</sup>
220 °C/16 h	40.0 ± 2.8 <sup>C,b,**</sup>	9.6 ± 0.5 <sup>B,a,ns</sup>	18.8 ± 1.9 <sup>C,b,**</sup>	27.8 ± 3.0 <sup>A,b</sup>	5.0 ± 1.1 <sup>B,b,*</sup>	26.7 ± 8.4 <sup>B,b,**</sup>
240 °C/4 h	44.3 ± 3.9 <sup>A,d,**</sup>	10.2 ± 0.4 <sup>A,a,ns</sup>	21.8 ± 2.1 <sup>A,a,ns</sup>	23.4 ± 3.9 <sup>C,a</sup>	5.8 ± 0.9 <sup>A,b,*</sup>	37.0 ± 7.6 <sup>A,b,**</sup>
240 °C/8 h	40.0 ± 6.3 <sup>B,c,**</sup>	9.1 ± 0.9 <sup>B,b,sn</sup>	17.3 ± 2.0 <sup>B,b,**</sup>	28.1 ± 6.2 <sup>B,a</sup>	4.5 ± 1.4 <sup>B,b,**</sup>	24.1 ± 8.0 <sup>B,d,**</sup>
240 °C/16 h	34.8 ± 2.2 <sup>C,c,**</sup>	7.9 ± 0.7 <sup>C,b,ns</sup>	13.3 ± 2.0 <sup>C,c,**</sup>	33.9 ± 2.6 <sup>A,a</sup>	1.7 ± 0.6 <sup>C,c,**</sup>	6.0 ± 2.4 <sup>C,c,**</sup>

Values are mean ± SD ( $n = 15$ ). Different capital and lowercase letters within a column indicate significant difference among various durations ( $p < 0.05$ ) and temperatures ( $p < 0.05$ ), respectively. ns: non-significant; \*:  $p < 0.05$ ; \*\*:  $p < 0.01$ , compared with untreated Japanese cedar timber.

[37]. In contrast, the  $\Delta E^*$  value, which is affected mainly by the  $L^*$  value, increased with increasing treatment temperature and duration.

In general, the MOE and MOR of heat-treated timber may reduce strength and increase brittleness, which are major barriers limiting the use of heat-treated timbers for construction applications [1,37]. As shown in Table 3, the MOE and MOR ranged from 1.7 to 6.9 GPa and 6.0–61.8 MPa, respectively. Of those values, the MOE remained nearly constant in the mass loss range up to 8%, while for a mass loss of 14.3% (240 °C/8 h), the MOE was slightly decreased to 4.5 GPa. In contrast, the MOR decreased markedly as a function of mass loss. The hydrothermal treatment at 160–240 °C decreased the MOR values of the untreated Japanese cedar timbers by 11.6–89.6%. This result indicated that the flexural properties of timber decreased after hydrothermal treatment, especially under high temperatures and long durations. Similar results were also reported by Borůvka et al. [4], Altgen et al. [21], and Yang et al. [37]. Among all hydrothermal treatments, 200 °C/8 h was the optimal condition; the given timber not only showed MOR retention higher than 80% but was also much less hygroscopic than untreated timber.

To obtain more information on the effect of hydrothermal treatment conditions on the properties of Japanese cedar timber, PCA was conducted to derive the significant factors. Fig. 2A shows the score scatter plot of PC1 versus PC2, with a total variability of 66.4%. Distinct segregation and clustering were apparent between different treatment conditions. Three groups could be observed based on the score scatter plot: one for untreated timbers, another for 240 °C/8 h, and a third for other hydrothermal treatments, which were affected mainly by the difference in PC1. These differentiations most likely reflect the main changes in the mass loss, pressure, MEE,  $\Delta E^*$  value, and EMC (Fig. 2B). Moreover, the PC1 loading of the treatment pressure was larger than the treatment temperature and duration. At the same time, the directions of

treatment pressure and mass loss overlapped, suggesting that the treatment pressure has a greater correlation than the treatment temperature and duration in hydrothermal treatment.

### 3.2. Chemical composition of untreated and hydrothermally treated Japanese cedar timbers

The PCA sequence of different treatment conditions and high total variability indicates that hydrothermal treatment follows a similar mechanism. Thus, the effect of various hydrothermal treatments on the chemical compositions of Japanese cedar timber was characterized by the original and second derivative ATR-FTIR spectra, as shown in Fig. 3. To compare the spectra of untreated and hydrothermally treated timbers, all spectra were normalized to the deformation peak at 1025  $\text{cm}^{-1}$ . Meanwhile, for a more accurate comparison of wavenumber changes, the peaks in the fingerprint region (1800–750  $\text{cm}^{-1}$ ) of the second derivative ATR-FTIR spectra are summarized in Table S1. The peak at 1025  $\text{cm}^{-1}$  was nearly constant in most treatments, but the peak of 240 °C/16 h was still highly variable, making 240 °C/16 h unsuitable for exploration in this way.

As shown in Table S1, the bands at 1736  $\text{cm}^{-1}$  were assigned to the stretching of the carbonyl groups of acetyls in hemicellulose. When timbers were under hydrothermal treatment, the intensities decreased with increasing treatment temperatures and durations. Compared with our previous study [38], the peak of ester carbonyl groups was not shifted to lower wavenumbers, which indicated that the hydroxyl groups did not form new carbonyl groups by esterification reactions. This result was similar to the result reported by Tjeerdsma and Militz [17], suggesting that the hydrothermal treatment was more similar to the heat treatment under an air atmosphere than under a nitrogen atmosphere. Furthermore, the intensity of the asymmetric ring stretching

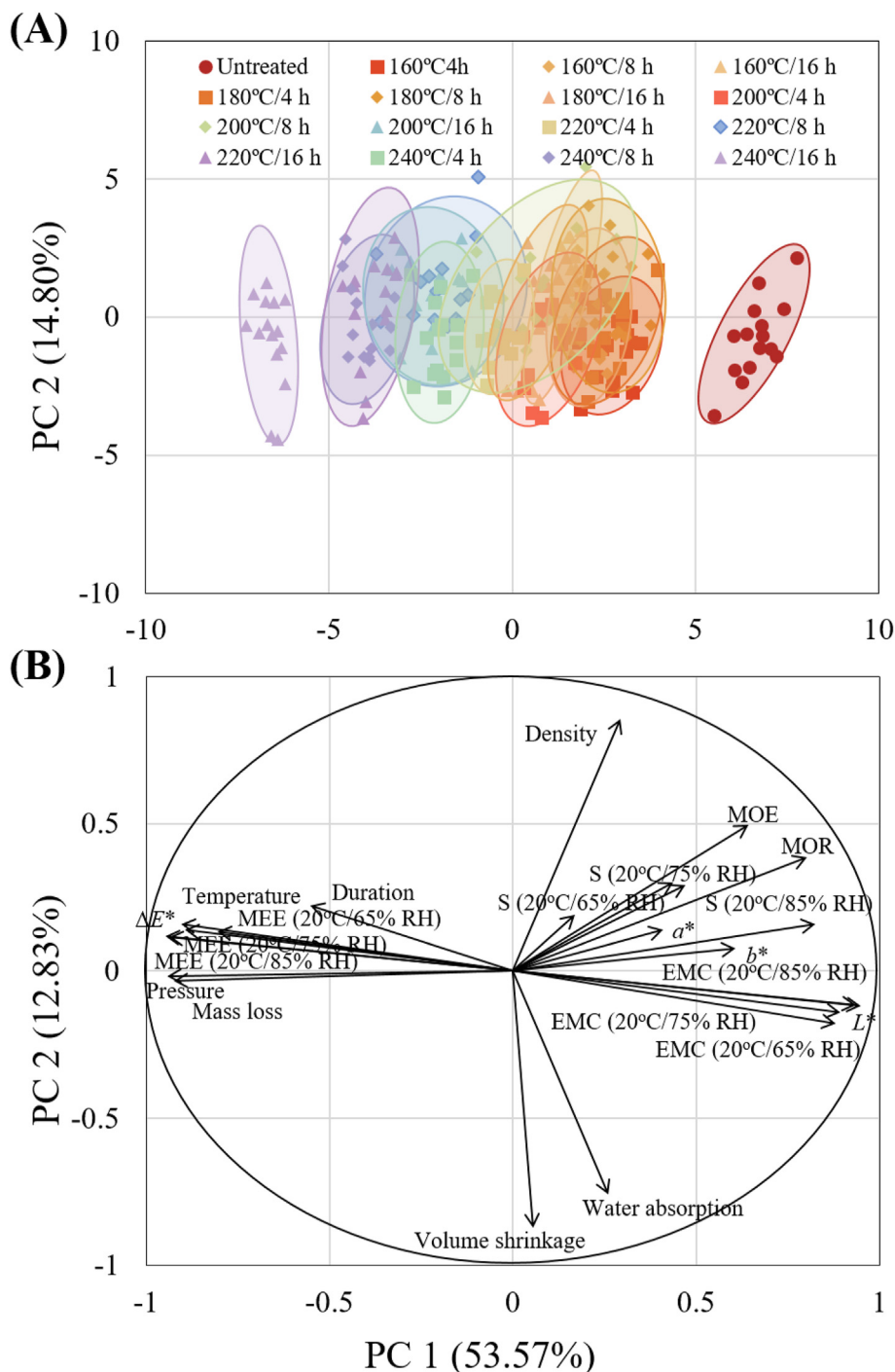


**Fig. 2 – Principal component analysis (A) and criteria selected (B) of untreated and hydrothermally treated Japanese cedar timber ( $n = 240$ ). EMC: equilibrium moisture content, MEE: moisture excluding efficiency, S: volumetric swelling coefficient, TVS: total volume swelling, MOE: modulus of elasticity, and MOR: modulus of rupture.**

band of cellulose at  $897\text{ cm}^{-1}$  was slightly reduced, which implied that cellulose was depolymerized during hydrothermal treatment. However, the standard deviation of aromatic skeletal stretching absorbance in lignin that appeared at  $1593\text{ cm}^{-1}$  was higher than the standard deviation of aromatic skeletal stretching absorbance in other peaks, probably because the timbers were conditioned at  $20\text{ }^{\circ}\text{C}/65\% \text{ RH}$  for 2

weeks instead of oven drying; thus, the spectrum was interfered with by the adsorbed water. In addition, the intensity of absorption peaks at  $1509\text{ cm}^{-1}$  (stretching of guaiacyl rings) and  $1265\text{ cm}^{-1}$  (guaiacyl ring breathing with C=O stretching, C–O stretching in lignin, and C–O linkage in guaiacyl aromatic methoxyl groups) showed a trend of first decreasing and then increasing with the intensification of hydrothermal

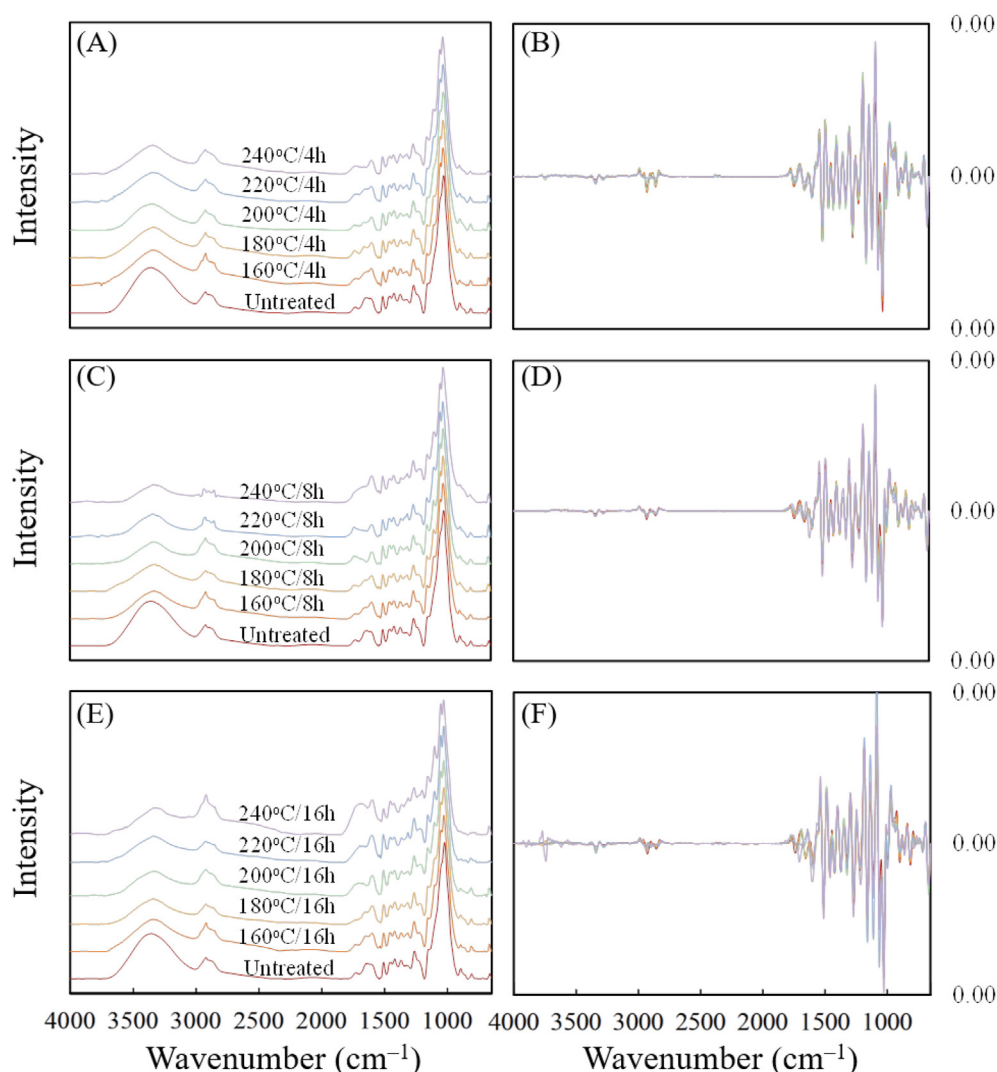


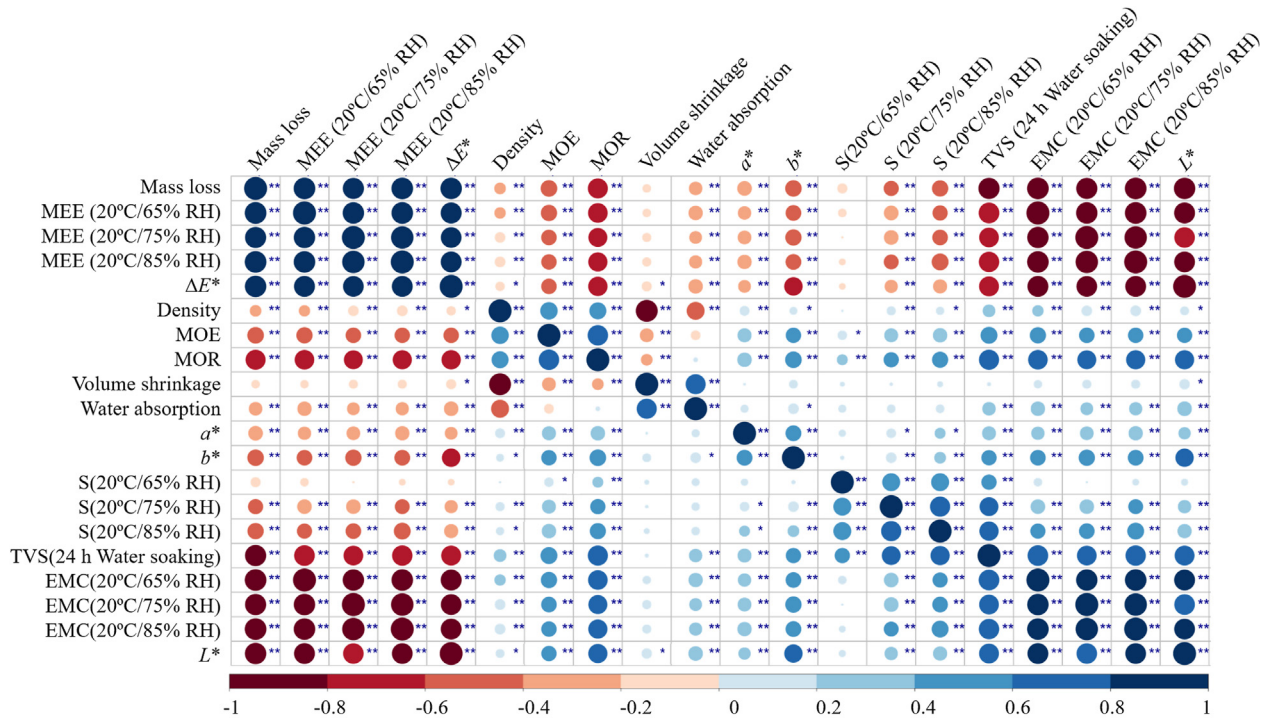
**Fig. 3 – Original and second derivative ATR-FTIR spectra of Japanese cedar timber after hydrothermal treatment at different temperatures for 4 h (A, B), 8 h (C, D), and 16 h (E, F).**

treatment. This phenomenon is attributed mainly to the initial thermal degradation temperature of lignin (110 °C) being lower than the initial thermal degradation temperature of hemicellulose (160 °C) [39], so the relative amount of lignin will also first decrease and then increase with the intensification of hydrothermal treatment. However, according to our previous study [39], the peaks at 1509 and 1265  $\text{cm}^{-1}$  increased up to 220 °C and then decreased at 260 °C under nitrogen or air atmospheres during heat treatment. This difference suggested that the water vapour of hydrothermal treatment may act as a protective medium for hemicellulose and cellulose, resulting in milder thermal degradation in the initial state. Additionally, the absorption peaks at 1460  $\text{cm}^{-1}$  ( $\delta$  C–H), 1218  $\text{cm}^{-1}$  ( $\nu$  C–O), and 863  $\text{cm}^{-1}$  ( $\delta$  C–H) were similar to the variation trend of guaiacol stretching vibration at 1509  $\text{cm}^{-1}$ , while the peaks at 1420  $\text{cm}^{-1}$  ( $\delta$  C–H) and 1320  $\text{cm}^{-1}$  ( $\delta$  CH<sub>2</sub>) showed opposite trends. Moreover, similar to the report of Tjeerdsma and Militz [17], the peaks in the fingerprint region did not shift significantly after hydrothermal treatment. The

findings suggested that the hydrothermal treatment limited and prevented shear displacement of the cell wall by promoting cellulose aggregation and hydrogen bonding rather than promoting additional covalent bonds and cross-linking. This result was also consistent with the reports of Popescu et al. [40].

### 3.3. Spearman's correlation matrix

To understand the effects of hydrothermal treatment on physicomechanical properties, chemical compositions, and their correlations, Spearman's correlation analysis was used in this study. Fig. 4 presents Spearman's correlation matrix of the selected properties. The diagonal elements (correlations of variables with themselves) are always equal to unity, and the correlation factors are between  $-1$  and  $1$  ( $0$ : no correlation;  $\pm 1$ : high correlation). For all physicomechanical properties, the mass loss was the most significantly correlated with the other properties. The mass loss not only denotes the density change



31

**Fig. 4 – Spearman's correlation matrix of the physicochemical properties of untreated and hydrothermally treated Japanese cedar timber ( $n = 240$ ). EMC: equilibrium moisture content, MEE: moisture excluding efficiency, S: volumetric swelling coefficient, TVS: total volume swelling, MOE: modulus of elasticity, and MOR: modulus of rupture. \*:  $p < 0.05$ ; \*\*:  $p < 0.01$ .**

after hydrothermal treatment but also indirectly reflects the hydrothermal degradation of the principal components. Additionally, the mass loss of hydrothermally treated timber generally increased with increasing treatment temperature and duration and was therefore often referred to as an indicator of treatment quality.

However, the main effect of the hydrothermal treatment is to reduce the hygroscopicity, thereby decreasing the swelling and shrinkage of timber by reducing its EMC. Therefore, the EMC, MEE, and S have significant correlations with each other, and a similar result was reported by Nopens et al. [41]. Notably, Spearman's correlation coefficient of hygroscopicity increased with increasing relative humidity, probably due to the increase in mechanical relaxation and the resoftening at higher relative humidity. Similar to the hygroscopicity, the mechanical properties also have significant correlations with other properties, such as mass loss, density, MEE, TVS, and EMC. Additionally, water absorption is significantly related to volume shrinkage, probably because the hydrothermal treatment reduces the density, leading to an increase in porosity [42]. Furthermore, consistent with the results reported by Van Nguyen et al. [43], there were significant correlations among the CIE  $L^*a^*b^*$  colour parameters, MEE, MOR, and EMC, which could be used for quality control in hydrothermal treatment.

Fig. 5 presents the Spearman's correlation matrix of the selected properties with the second derivative ATR-FTIR spectra. The specific hemicellulose acetyl group at

$1736\text{ cm}^{-1}$  was significantly associated with the mass loss, MEE,  $\Delta E^*$  value, S, EMC, MOE, MOR, and  $L^*$  value. This result suggested that the products generated from the degradation (deacetylation) of hemicellulose play an important catalytic role in the hydrothermal process. Additionally, the structural features of cellulose have a great influence on the mechanical properties, resulting in the peak at  $897\text{ cm}^{-1}$  ( $\nu_{\text{as}}\text{ C-O-C}$ ,  $\beta$ -(1-4)-glycosidic linkage) being significantly correlated with the mechanical properties. In contrast, the relative content of lignin increased due to the degradation of hydrophilic hemicellulose. Therefore, the specific absorption peaks of lignin at  $1593$ ,  $1509$ , and  $1265\text{ cm}^{-1}$  were negatively correlated with MEE. Similarly, the signals at  $1320\text{ cm}^{-1}$  ( $\delta\text{ CH}_2$ ),  $1156\text{ cm}^{-1}$  ( $\nu_{\text{as}}\text{ C-O-C}$ ,  $\delta\text{ C-O-H}$ ),  $1107\text{ cm}^{-1}$  ( $\nu\text{ C-C}$ ,  $\text{C-O}$ ,  $\delta\text{ C-O-H}$ ), and  $1060\text{ cm}^{-1}$  ( $\nu\text{ C-C}$ ,  $\text{C-O}$ ,  $\delta\text{ C-O-H}$ ) were also negatively correlated with MEE. In addition to the chemical changes described in the previous section, the water absorption and volume shrinkage were significantly correlated to  $1593$ ,  $1509$ ,  $1460$ ,  $1265$ ,  $1218$ , and  $863\text{ cm}^{-1}$ . Previous work has shown that degradation of hemicellulose is correlated with improved anti-shrinkage ability of lignocellulosic materials [44], but compared with hemicellulose and cellulose, the changes in volume shrinkage and water absorption were more related to the relative content of lignin according to Spearman's correlation analysis in this study. The initial thermal degradation temperature of lignin is well known to be lower than the initial thermal degradation temperature of hemicellulose and

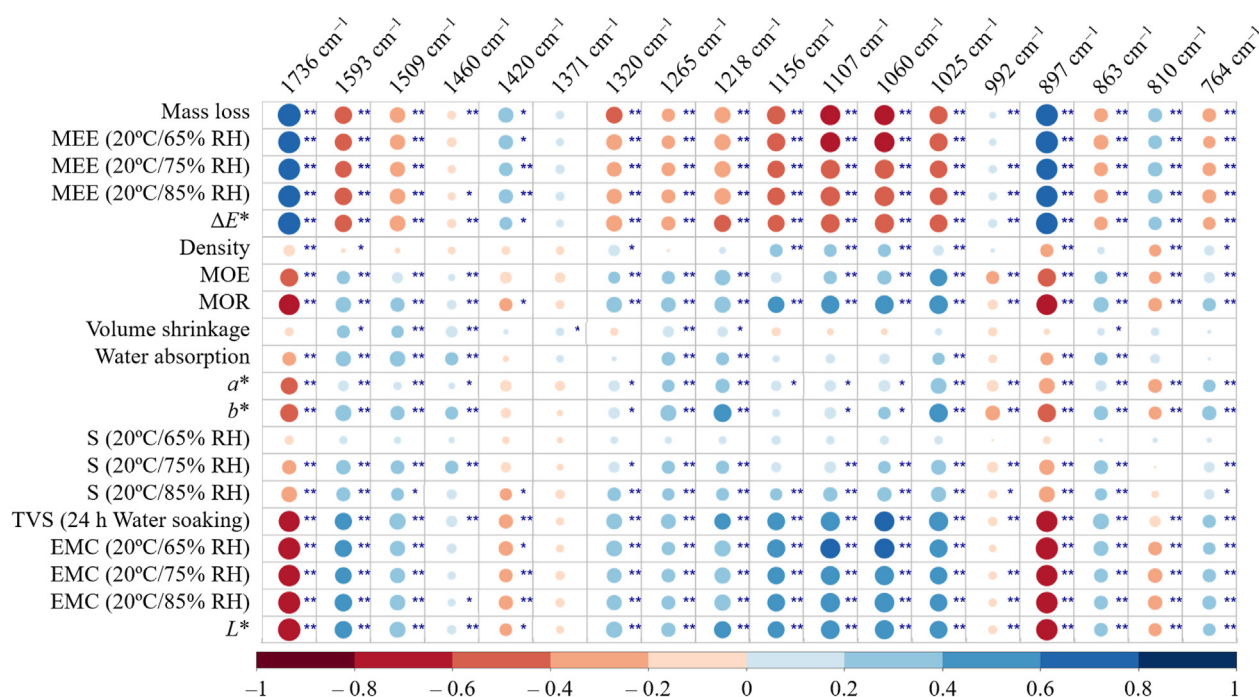


**Fig. 5 – Spearman's correlation matrix of physicochemical properties with second derivative ATR-FTIR spectra of untreated and hydrothermally treated Japanese cedar timber ( $n = 240$ ). EMC: equilibrium moisture content, MEE: moisture excluding efficiency, S: volumetric swelling coefficient, TVS: total volume swelling, MOE: modulus of elasticity, and MOR: modulus of rupture. \*:  $p < 0.05$ ; \*\*:  $p < 0.01$ .**

cellulose. The slight changes in volume shrinkage and water absorption after hydrothermal treatment may be caused by the thermal energy released from lignin during pyrolysis along with the formation of microcracks [45]. El Moustaqim et al. [46] also mentioned that stress relaxation of lignin can lead to microcracks. However, the volume shrinkage and water absorption decreased with increasing treatment temperature and duration, attributed to the hydrothermal treatment not only destroyed the lignin structure but also lowered the lignin glass transition temperature, making it easier to deposit on the cell wall surface [47–49].

#### 4. Conclusions

To understand the processes involved in hydrothermal treatment, this study investigated the physicochemical properties and chemical composition of hydrothermally treated Japanese cedar timber. The results revealed that the hygroscopicity and flexural properties generally decreased with increasing treatment temperature and duration. The mechanical properties and dimensional stability are important factors in determining the application of heat-treated timber in outdoor and building structures. In this study, 200 °C/8 h was the optimal condition among all treatments; the given timber not only retained  $\geq 80\%$  of its flexural strength but was also much less hygroscopic than untreated

timber. Additionally, the results of Spearman's correlation test revealed that hemicellulose and cellulose were significantly related to mass loss, MEE, EMC, and MOR. In contrast, lignin was more associated with volume shrinkage and water absorption. The hydrothermal treatment limited and prevented shear displacement of the cell wall by promoting cellulose aggregation and hydrogen bonding, thereby reducing the possibility of cracking and the degradation of mechanical properties. Therefore, appropriate hydrothermal treatment conditions may become an environmentally friendly method for timber modification.

#### Declaration of competing interest

The authors declare the following financial interests/personal relationships which may be considered as potential competing interests: Jyh-Horng Wu reports financial support was provided by Forestry Bureau of the Council of Agriculture, Taiwan.

#### Acknowledgments

This work was financially supported by a research grant from the Forestry Bureau of the Council of Agriculture, Taiwan [grant number 111AS-7.4.4-FB-e2(3)].

## Appendix A. Supplementary data

Supplementary data to this article can be found online at <https://doi.org/10.1016/j.jmrt.2022.11.092>.

### REFERENCES

- [1] Čekovská H, Gaff M, Osvald A, Kačík F, Kubš J, Kaplan L. Fire resistance of thermally modified spruce wood. *Bioresources* 2017;12(1):947–59.
- [2] Rasdianah D, Zaidon A, Hidayah A, Lee SH. Effects of superheated steam treatment on the physical and mechanical properties of light red meranti and kedondong wood. *J Trop For Sci* 2018;30(3):384–92.
- [3] Fu Z, Zhou Y, Gao X, Liu H, Zhou F. Changes of water related properties in radiata pine wood due to heat treatment. *Construct Build Mater* 2019;227:116692.
- [4] Borůvka V, Dudík R, Zeidler A, Holeček T. Influence of site conditions and quality of birch wood on its properties and utilization after heat treatment. Part I–Elastic and strength properties, relationship to water and dimensional stability. *Forests* 2019;10(2):189.
- [5] He Z, Qian J, Qu L, Yan N, Yi S. Effects of Tung oil treatment on wood hygroscopicity, dimensional stability and thermostability. *Ind Crop Prod* 2019;140:111647.
- [6] Lee SH, Ashaari Z, Lum WC, Halip JA, Ang AF, Tan LP, et al. Thermal treatment of wood using vegetable oils: a review. *Construct Build Mater* 2018;181:408–19.
- [7] Meints T, Hansmann C, Müller M, Liebner F, Gindl-Altmutter W. Highly effective impregnation and modification of spruce wood with epoxy-functional siloxane using supercritical carbon dioxide solvent. *Wood Sci Technol* 2018;52(6):1607–20.
- [8] Mantanis GI. Chemical modification of wood by acetylation or furfurylation: a review of the present scaled-up technologies. *Bioresources* 2017;12(2):4478–89.
- [9] Digaitis R, Thybring EE, Thygesen LG, Fredriksson M. Targeted acetylation of wood: a tool for tuning wood-water interactions. *Cellulose* 2021;28(12):8009–25.
- [10] Endo R, Kamei K, Iida I, Kawahara Y. Dimensional stability of waterlogged wood treated with hydrolyzed feather keratin. *J Archaeol Sci* 2008;35(5):1240–6.
- [11] Tavassoli F, Razzaghi-Kashani M, Mohebbi B. Hydrothermally treated wood as reinforcing filler for natural rubber bio-composites. *J Polym Res* 2018;25(1):1–11.
- [12] Ali MR, Abdullah UH, Ashaari Z, Hamid NH, Hua LS. Hydrothermal modification of wood: a review. *Polymers* 2021;13(16):2612.
- [13] Kyyrö S, Altgen M, Seppäläinen H, Belt T, Rautkari L. Effect of drying on the hydroxyl accessibility and sorption properties of pressurized hot water extracted wood. *Wood Sci Technol* 2021;55(5):1203–20.
- [14] Herrera-Builes JF, Sepúlveda-Villarroel V, Osorio JA, Salvo-Sepúlveda L, Ananíás RA. Effect of thermal modification treatment on some physical and mechanical properties of pinus oocarpa wood. *Forests* 2021;12(2):249.
- [15] Hakkou M, Pétrissans M, Gérardin P, Zoulalian A. Investigations of the reasons for fungal durability of heat-treated beech wood. *Polym Degrad Stabil* 2006;91(2):393–7.
- [16] Jirouš-Rajković V, Miklečić J. Heat-treated wood as a substrate for coatings, weathering of heat-treated wood, and coating performance on heat-treated wood. *Adv Mater Sci Eng* 2019;2019:8621486.
- [17] Tjeerdma BF, Militz H. Chemical changes in hydrothermal treated wood: FTIR analysis of combined hydrothermal and dry heat-treated wood. *Holz Roh Werkst* 2005;63(2):102–11.
- [18] Windeisen E, Strobel C, Wegener G. Chemical changes during the production of thermo-treated beech wood. *Wood Sci Technol* 2007;41(6):523–36.
- [19] Wang D, Fu F, Lin L. Molecular-level characterization of changes in the mechanical properties of wood in response to thermal treatment. *Cellulose* 2022;29:3131–42.
- [20] Čermák P, Baar J, Dömény J, Výbohá E, Rousek R, Pařil P, et al. Wood-water interactions of thermally modified, acetylated and melamine formaldehyde resin impregnated beech wood. *Holzforschung* 2022;76(5):437–50.
- [21] Altgen M, Uimonen T, Rautkari L. The effect of de- and re-polymerization during heat-treatment on the mechanical behavior of Scots pine sapwood under quasi-static load. *Polym Degrad Stabil* 2018;147:197–205.
- [22] CNS standard. 451. Wood – Determination of density for physical and mechanical tests. Taipei, Taiwan: Bureau of Standards, Metrology and Inspection; 2013.
- [23] CNS standard. 452. Wood – Determination of moisture content for physical and mechanical tests. Taipei, Taiwan: Bureau of Standards, Metrology and Inspection; 2013.
- [24] CNS standard. 14927. Wood – Determination of volumetric swelling. Taipei, Taiwan: Bureau of Standards, Metrology and Inspection; 2012.
- [25] ASTM standard. D1037–12. Standard test methods for evaluating properties of wood-base fiber and particle panel materials. West Conshohocken, PA: ASTM International; 2012.
- [26] CNS standard. 454. Wood – Determination of static bending properties. Taipei, Taiwan: Bureau of Standards, Metrology and Inspection; 2013.
- [27] Mansfield JR, Sowa MG, Scarth GB, Somorjai RL, Mantsch HH. Fuzzy C-means clustering and principal component analysis of time series from near-infrared imaging of forearm ischemia. *Comput Med Imag Graph* 1997;21:299–308.
- [28] Wei T, Simko V, Levy M, Xie Y, Jin Y, Zemla J. Package ‘corrplot. *Stat* 2017;56(316):e24.
- [29] Jeong SY, Lee JW. Hydrothermal treatment. In: Pandya A, Negi S, Binod P, Larroche C, editors. Pretreatment of biomass: processes and technologies. Elsevier; 2015. p. 61–74.
- [30] Rissanen JV, Grénman H, Willför S, Murzin DY, Salmi T. Spruce hemicellulose for chemicals using aqueous extraction: kinetics, mass transfer, and modeling. *Ind Eng Chem Res* 2014;53(15):6341–50.
- [31] Cai C, Javed MA, Komulainen S, Telkki VV, Haapala A, Heräjärvi H. Effect of natural weathering on water absorption and pore size distribution in thermally modified wood determined by nuclear magnetic resonance. *Cellulose* 2020;27(8):4235–47.
- [32] Wentzel M, Fleckenstein M, Hofmann T, Militz H. Relation of chemical and mechanical properties of Eucalyptus nitens wood thermally modified in open and closed systems. *Wood Mater Sci Eng* 2019;14(3):165–73.
- [33] Wentzel M, Koddenberg T, Militz H. Anatomical characteristics of thermally modified Eucalyptus nitens wood in an open and closed reactor system. *Wood Mater Sci Eng* 2020;15(4):223–8.
- [34] Bernabei M, Salvatici MC. In situ ESEM observations of spruce wood (*Picea abies* Karst.) during heat treatment. *Wood Sci Technol* 2016;50(4):715–26.
- [35] Altgen M, Willems W, Hosseinpourpia R, Rautkari L. Hydroxyl accessibility and dimensional changes of Scots pine sapwood affected by alterations in the cell wall ultrastructure during heat-treatment. *Polym Degrad Stabil* 2018;152:244–52.

- [36] Endo K, Obataya E, Zeniya N, Matsuo M. Effects of heating humidity on the physical properties of hydrothermally treated spruce wood. *Wood Sci Technol* 2016;50(6):1161–79.
- [37] Yang TH, Chang FR, Lin CJ, Chang FC. Effects of temperature and duration of heat treatment on the physical, surface, and mechanical properties of Japanese cedar wood. *Bioresources* 2016;11(2):3947–63.
- [38] Chien YC, Yang TC, Hung KC, Li CC, Xu JW, Wu JH. Effects of heat treatment on the chemical compositions and thermal decomposition kinetics of Japanese cedar and beech wood. *Polym Degrad Stabil* 2018;158:220–7.
- [39] Orfão JJM, Antunes FJA, Figueiredo JL. Pyrolysis kinetics of lignocellulosic materials—three independent reactions model. *Fuel* 1999;78(3):349–58.
- [40] Popescu CM, Navi P, Peña MIP, Popescu MC. Structural changes of wood during hydro-thermal and thermal treatments evaluated through NIR spectroscopy and principal component analysis. *Spectrochim Acta, Part A* 2018;191:405–12.
- [41] Nopens M, Riegler M, Hansmann C, Krause A. Simultaneous change of wood mass and dimension caused by moisture dynamics. *Sci Rep* 2019;9(1):1–11.
- [42] Zauer M, Pfriem A, Wagenführ A. Toward improved understanding of the cell-wall density and porosity of wood determined by gas pycnometry. *Wood Sci Technol* 2013;47(6):1197–211.
- [43] Van Nguyen TH, Nguyen TT, Ji X, Guo M. Predicting color change in wood during heat treatment using an artificial neural network model. *Bioresources* 2018;13(3):6250–64.
- [44] Lou Z, Yuan T, Wang Q, Wu X, Hu S, Hao X, et al. Fabrication of crack-free flattened bamboo and its macro-/micromorphological and mechanical properties. *J Review Mater* 2021;9(5):959.
- [45] Kifani-Sahban F, Kifani A, Belkbir L, Belkbir A, Zoulalian A, Arauzo J, et al. A physical approach in the understanding of the phenomena accompanying the thermal treatment of lignin. *Thermochim Acta* 1997;298(1–2):199–204.
- [46] El Moustaqim M, El Kaihal A, El Marouani M, Men-La-Yakhaf S, Taibi M, Sebbahi S, et al. Thermal and thermomechanical analyses of lignin. *Sustain Chem Pharm* 2018;9:63–8.
- [47] Li H, Pu Y, Kumar R, Ragauskas AJ, Wyman CE. Investigation of lignin deposition on cellulose during hydrothermal pretreatment, its effect on cellulose hydrolysis, and underlying mechanisms. *Biotechnol Bioeng* 2014;111(3):485–92.
- [48] Xiao LP, Lin Z, Peng WX, Yuan TQ, Xu F, Li NC, et al. Unraveling the structural characteristics of lignin in hydrothermal pretreated fibers and manufactured binderless boards from *Eucalyptus grandis*. *Sustain Chem Process* 2014;2(1):1–12.
- [49] Pelaez-Samaniego MR, Yadama V, Garcia-Perez M, Lowell E, McDonald AG. Effect of temperature during wood torrefaction on the formation of lignin liquid intermediates. *J Anal Appl Pyrol* 2014;109:222–33.